Laboratory Tests of Low Density Astrophysical Nuclear Equations of State

L. Qin,[1] K. Hagel,[1] R. Wada,[2,1] J. B. Natowitz,[1] S. Shlomo,[1] A. Bonasera,[1,3] G. Röpke,[4] S. Typel,[5] Z. Chen,[6] M. Huang,[6]
J. Wang,[6] H. Zheng,[1] S. Kowalski,[7] M. Barbui,[1] M. R. D. Rodrigues,[1] K. Schmidt,[1] D. Fabris,[8] M. Lunardon,[8] S. Moretto,[8]
G. Nebbia,[8] S. Pesente,[8] V. Rizzi,[8] G. Viesti,[8] M. Cinausero,[9] G. Prete,[9] T. Keutgen,[10] Y. El Masri,[10]
Z. Majka,[11] and Y. G. Ma[12]

[1]*Cyclotron Institute, Texas A&M University, College Station, Texas 77843, USA*
[2]*Institute of Modern Physics HIRFL, Chinese Academy of Sciences, Lanzhou, 730000, China*
[3]*Laboratori Nazionali del Sud, INFN, via Santa Sofia, 62, 95123 Catania, Italy*
[4]*University of Rostock, FB Physik, Rostock, Germany*
[5]*GSI Helmholtzzentrum fur Schwerionenforschung GmbH, Theorie, Planckstraße 1, D-64291 Darmstadt, Germany*
[6]*Institute of Modern Physics HIRFL, Chinese Academy of Sciences, Lanzhou, 730000, China*
[7]*Institute of Physics, Silesia University, Katowice, Poland*
[8]*Dipartamento di Fisica dell Universita di Padova and INFN Sezione di Padova, Padova, Italy*
[9]*INFN Laboratori Nazionali di Legnaro, Legnaro, Italy*
[10]*FNRS and IPN, Université Catholique de Louvain, B-1348 Louvain-Neuve, Belgium*
[11]*Smoluchowski Institute of Physics, Jagiellonian University, Krakow, Poland*
[12]*Shanghai Institute of Nuclear Research, Chinese Academy of Sciences, Shanghai 201800, China*
(Received 22 October 2011; published 24 April 2012)

Clustering in low density nuclear matter has been investigated using the NIMROD multidetector at Texas A&M University. Thermal coalescence modes were employed to extract densities, ρ, and temperatures, T, for evolving systems formed in collisions of $47A$ MeV ^{40}Ar + ^{112}Sn, ^{124}Sn and ^{64}Zn + ^{112}Sn, ^{124}Sn. The yields of d, t, ^{3}He, and ^{4}He have been determined at $\rho = 0.002$ to 0.03 nucleons/fm^3 and $T = 5$ to 11 MeV. The experimentally derived equilibrium constants for α particle production are compared with those predicted by a number of astrophysical equations of state. The data provide important new constraints on the model calculations.

Introduction.—A reliable understanding of the nuclear equation of state (EOS) over a wide range of densities and temperatures is crucial to both nuclear science and to our understanding of stellar evolution and supernovae [1]. In the latter context, it is well known that a valid treatment of the correlations and clusterization in low density matter is a vital ingredient of astrophysical models. To meet the need for the nuclear input, some extensive well known calculations and existing tabulations, based on varying effective interactions, were developed and have served as standard input for a wide variety of astrophysical simulations [2–4]. More recently some new approaches have led to a number of new predictions [5–10]. While all of the models in use lead to strong alpha clustering of the matter at low nucleon densities, ρ, and temperatures, T, they differ significantly in their quantitative predictions, usually tabulated as alpha mass fractions, at specified T, ρ, and proton mass fraction, Y_P. See references [7,9], for example. For a given Y_P the differences in the absolute values reflect differences in the effective interactions inherent in the chosen nuclear equation of state, differences in the formulation and approximations employed in the models, and differences in the treatment of possible competing species. We present here results of an experimental determination of clustering yields in low density nuclear matter and use these results to make a direct test of the different models, focusing on

alpha clustering. Our test observable is not the alpha mass fraction but rather the equilibrium constant for alpha particle clustering. The model derived equilibrium constants should be nearly independent of proton fraction and the choice of competing species assumed in a particular model.

Experimental techniques.—We reported in Refs. [11,12] that measurements of nucleon and light cluster emission from the participant matter which is produced in near Fermi energy heavy ion collisions could be employed to probe the EOS at low densities and moderate temperatures where clustering is important. Our data demonstrated a large degree of alpha clustering for densities at and below ~ 0.05 times normal nuclear density and temperatures of 4 to 10 MeV. Using these data we derived experimental symmetry free energies in low density nuclear matter [11,12]. That analysis employed the isoscaling technique which compares yields for two systems with similar temperatures but different N/Z ratios to determine the differences in chemical potentials and symmetry energy [13,14].

The NIMROD 4π multidetector at Texas A&M University has now been used to extend our clustered matter measurements to higher densities. Cluster production in collisions of $47A$ MeV ^{40}Ar with ^{112,124}Sn and ^{64}Zn with ^{112,124}Sn was studied. NIMROD consists of a 166 segment charged particle array set inside a neutron ball [15]. The

charged particle array is arranged in 12 rings of Si-CsI telescopes or single CsI detectors concentric around the beam axis. The CsI detectors are 1–10 cm thick Tl doped crystals read by photomuliplier tubes. A pulse shape discrimination method is employed to identify light particles in the CsI detectors. For this experiment, each of the forward rings included two segments having two Si detectors (150 and 500 μm thick) in front of the CsI detectors (super telescopes) and three having one Si detector (300 μm thick). Each super telescope was further divided into two sections. Neutron multiplicity was measured with the 4π neutron detector surrounding the charged particle array. This detector is a neutron calorimeter filled with Gd doped pseudocumene. Thermalization and capture of emitted neutrons in the ball leads to scintillation which is observed with phototubes providing event by event determinations of neutron multiplicity. Further details on the detection system, energy calibrations and neutron ball efficiency may be found in Ref. [16]. The combined neutron and charged particle multiplicities were employed to select the most violent events for subsequent analysis.

Analysis.—The dynamics of the collision process allow us to probe the nature of the intermediate velocity "nucleon-nucleon" emission source [17–19]. Measurement of emission cross sections of nucleons and light clusters together with suitable application of a coalescence ansatz [20] provides the means to probe the properties and evolution of the interaction region. The techniques used have been detailed in several previous publications [11,12,17–19] and are described briefly below. A notable difference from Refs. [11,12] is the method of density extraction. This is discussed more extensively in the following. We emphasize that the event election is on the more violent collisions. Cross section weighting favors midrange impact parameters.

An initial estimation of emission multiplicities at each stage of the reaction was made by fitting the observed light particle spectra assuming contributions from three sources, a projectilelike fragment source, an intermediate velocity (IV) source, and a targetlike fragment source. A reasonable reproduction of the observed spectra is achieved. Except for the most forward detector rings the data are dominated by particles associated with the IV and targetlike fragment sources. The IV source velocities are very close to 50% of the beam velocity as seen in many other studies [17–19]. The observed spectral slopes reflect the evolution dynamics of the source [17,21,22]. For further analysis, this IV source is most easily sampled at the intermediate angles where contributions from the other sources are minimized. For the analysis of the evolution of the source we have selected the data in ring 9 of the NIMROD detector. This ring covered an angular range in the laboratory of 38° to 52°. Inspection of invariant velocity plots constructed for each ejectile and each system, as well as of the results of the three-source fit analyses indicate that this selection of

angular range minimizes contributions from secondary evaporative decay of projectilelike or targetlike sources. We treat the IV source as a nascent fireball created in the participant interaction zone.

The expansion and cooling of this zone leads to a correlated evolution of density and temperature which we probe using particle and cluster observables, yield, energy, and angle. As in the previous work [11,12], we have employed double isotope yield ratios [23,24] to characterize the temperature at a particular emission time. Model studies comparing Albergo model [23] temperatures and densities to the known input values have shown the double isotope ratio temperatures to be relatively robust in this density range [25]. However, the densities extracted using the Albergo model are useful only at the very lowest densities [25]. Consequently, in this study we have employed a different means of density extraction, the thermal coalescence model of Mekjian [17,20].

To determine the coalescence parameter P_0, the radius in momentum space, from our data we have followed the Coulomb-corrected coalescence model formalism of Awes *et al.* [26] and previously employed by us in Ref. [17]. In the laboratory frame the derived relationship between the observed cluster and proton differential cross sections is

$$\frac{d^2N(Z,N,E_A)}{dE_A d\Omega} = R_{np}^N \frac{A^{-1}}{N!Z!}\left(\frac{4\pi P_0^3}{3[2m^3(E-E_C)]^{1/2}}\right)^{A-1}$$
$$\times\left(\frac{d^2N(1,0,E)}{dEd\Omega}\right)^A, \qquad (1)$$

where the double differential multiplicity for a cluster of mass number A containing Z protons and N neutrons and having a Coulomb-corrected energy E_A, is related to the proton double differential multiplicity at the same Coulomb-corrected energy per nucleon, $E - E_C$, where E_C is the Coulomb barrier for proton emission. R_{np} is the neutron to proton ratio.

A strict quantitative application of the coalescence model requires knowledge of cluster, neutron, and proton differential cross sections with proper absolute normalizations. In this work absolute measured multiplicities for the selected violent events are employed. The neutron spectra are not measured. However, since within the framework of the coalescence model the yield ratios of two isotopes which differ by one neutron are determined by their binding energies and the n/p ratio in the coalescence volume, we have used the observed triton to ^{3}He yield ratio to derive the n/p ratio used in this analysis.

In the Mekjian model thermal and chemical equilibrium determines coalescence yields of all species. Under these assumptions there is a direct relationship between the derived radius in momentum space and the volume of the emitting system. In terms of the P_0 derived from Eq. (1) and assuming a spherical source,

$$V = \frac{3h^3}{4\pi P_0^3}\left[(2s+1)\left(\frac{Z!N!A^3}{2^A}\right)e^{E_0/T}\right]^{1/(A-1)}, \quad (2)$$

where h is Planck's constant and Z, N, and A are the same as in Eq. (1). E_0 is the binding energy, s the spin of the emitted cluster, and T is the temperature. Thus, the radius, and therefore the volume, can be derived from the observed P_0 and temperature values assuming a spherical shape. We note that this volume is a free volume.

Because our goal was to derive information on the density and temperature evolution of the emitting system, our analysis was not limited to determining an average P_0 value. Instead, as in our previous studies [17], results for d, t, ^{3}He, and ^{4}He, were derived as a function of v_{surf}, the velocity of the emerging particle at the nuclear surface, prior to Coulomb acceleration. From the relevant P_0 values we then determined volumes using Eq. (2). A comparison of these volumes indicated good agreement for t, ^{3}He and ^{4}He. The volumes derived from the deuteron data are typically somewhat smaller. This appears to reflect the fragility of the deuteron and its survival probability once formed [27]. For this reason, we have used average volumes derived from the $A > 2$ clusters in the analysis. Given that mass is removed from the system during the evolution, we determined the relevant masses for each volume by assuming that the initial mass of the source was that obtained in the source fitting analysis and then deducing the mass remaining at a given v_{surf} from the observed energy spectra. This is also an averaging process and ignores fluctuations. Once these masses were known they were used to determine an excluded volume for the particles. Addition of this excluded volume to the free volume produced the total volumes needed for the density calculations. These were determined by dividing the mass remaining by the total volume. This was done as a function of v_{surf}.

Results.—

*Temperatures and densities.—*Inspection of the results for the four different systems studied revealed that the temperatures, densities, and equilibrium constants for all systems are the same within statistical uncertainties. Therefore, we have combined them to determine the values reported in this Letter.

We present in Fig. 1 the experimentally derived density and temperature evolution of the IV source. Densities are expressed as total number of nucleons (including those in clusters) per fm^3. There is a strong correlation of increasing temperature with increasing density.

Estimated errors on these temperatures are 10% below $\rho = 0.01$ increasing to 15% at $\rho \sim 0.03$. The error in the derivation of the density arises from the uncertainty on the volume which is dominated by the uncertainty in temperature and the uncertainty in source mass derived from source fitting to complex spectra. The estimated errors are $\pm 17\%$. We have included in each figure shaded bands representing this uncertainty in density. On the log plot the uncertainties in K are much smaller.
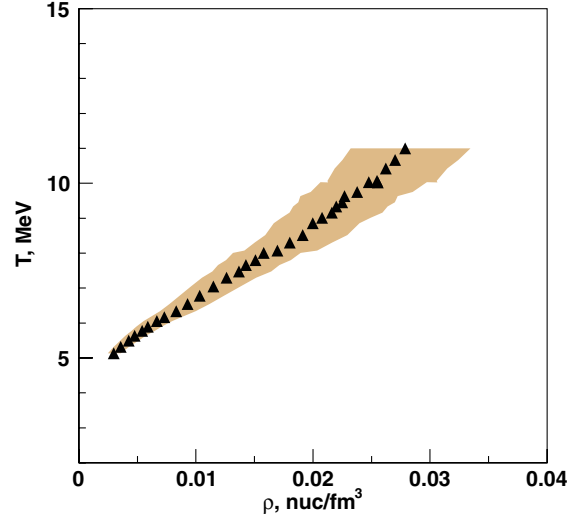

FIG. 1 (color online).   Temperatures and densities sampled by the expanding IV source. The shaded band indicates the uncertainty in density. See text.

*Equilibrium constants.—*As already mentioned above, the absolute cluster yields and mass fractions calculated by the models depend upon the N/Z ratio of the matter, the model specific nucleon-nucleon interaction assumed, and the various approximations of a given model. In addition, as all of the treatments assume chemical equilibrium, they also depend upon the number and type of competitive species included in the calculation. Historically, most EOS tables, used in astrophysical simulations, have treated only neutrons, protons, α particles, and a single average heavy nucleus [2,3]. More recently some models have been developed in which the number of competing species treated has been greatly expanded [8–10]. In an equilibrium situation, all relevant equilibria must be simultaneously satisfied. Thus, if relevant species are not included, the calculated mass fractions of all included species will be in error.

For this reason, we do not believe that a direct comparison with calculated mass fractions is the appropriate way to test the individual models. We choose, rather, to compare the experimentally derived equilibrium constants for the production of α particles with those of the models. The model derived equilibrium constants should be independent of proton fraction and the choice of competing species in a particular model. Specifically we define the equilibrium constant, K_c, as

$$K_c(A, Z) = \frac{\rho(A, Z)}{\rho_p^Z \rho_n^{(A-Z)}}, \quad (3)$$

where $\rho(A, Z)$, ρ_p, and ρ_n are, respectively, the densities of cluster of mass A and atomic number Z, free protons, and free neutrons. We express the densities in units of nucleons/fm^3. In Fig. 2, we present the equilibrium constants, K_c, for d, t, ^{3}He, and ^{4}He cluster formation
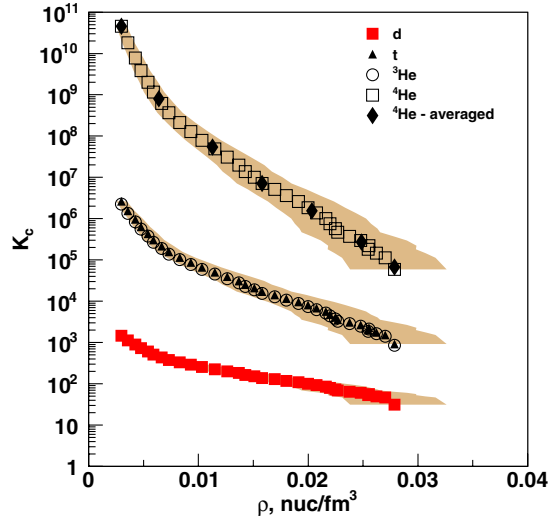
FIG. 2 (color online).   Equilibrium constants K_c derived from the experimental yields. See text. Solid squares: K_c (d), Solid triangles: K_c (t), Open circles: K_c (^{3}He) and open squares: K_c (α). Solid diamonds indicate the values of K_c (α) corresponding to integral values of the temperature from 5 to 11 MeV (left to right). The shaded bands indicate the uncertainty in density. See text.

FIG. 3 (color online).   Comparison of experimental values of K_c (α) with those from various EOS calculations. See text for the theoretical models. The shaded band indicates the uncertainty in density for the experimental data. See text.

as a function of density. For the purpose of later comparisons with EOS calculations, we have interpolated the experimental data for the alpha cluster to determine the equilibrium constants at integral temperatures from 5 to 11 MeV. These values are indicated by solid black diamonds on the figure. Temperatures increase as the density increases. Statistical errors are smaller than the symbols.

For the purposes of a general assessment of the available EOS calculations at low density, we present in Fig. 3 a comparison between the experimentally derived values of $K_c(\alpha)$ and those predicted by available astrophysical EOS calculations. Note that this plot is logarithmic in K_c. The solid black diamonds connected by a dashed line indicate the experimental results. For a further comparison we show with a dotted line the results of the Virial EOS of Horowitz and Schwenk [5]. This EOS is based on virial coefficients derived from scattering data and has been suggested as a benchmark for other calculations at low density. Not surprisingly the calculated values of the equilibrium constant tend to converge at the lower densities. Even at the lowest densities sampled, however, there are significant differences. At higher densities, 0.01 to 0.03 nuc/fm^3, the various interactions employed all lead to a decrease of K_c below that of the nuclear statistical equilibrium (NSE) values of Typel *et al.* [7] as expected. However there are significant differences in the models, both in absolute value and in the rate of change of $K_c(\alpha)$ at the higher densities. In the density range above $\sim$0.01 nuc/fm^3, the predictions of the virial model of Schwenk and Horowitz [5], the model of H. Shen *et al.* [2], the Lattimer Swesty model with a Skyrme interaction having an incompressibility of
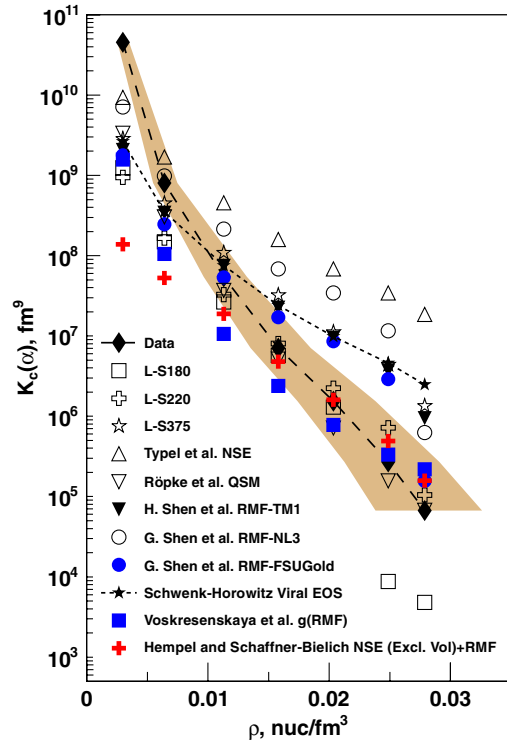
375 MeV [3] and those of G. Shen *et al.* which employ the FSUGold [10] or NL3 interaction [9] all exhibit shallower slopes than the data and values all well above the data.

The model predictions showing better agreement with the data above 0.01 nuc/fm^3 are the Lattimer and Swesty calculations employing Skyrme interactions with incompressibilities of 180 and 220 MeV [3]. They are close to the data except for the two points for 180 MeV at highest density.

The quantum statistical model (QSM) results are very close to the experimental results. The present calculations include the latest QSM estimates of momentum dependent in-medium binding energy shifts [7,28]. Although well below the data and the other model calculations at the lowest velocities, the results from Ref. [8], an NSE model which includes excluded volume effects are in good agreement with the data at the higher velocities. In a recent paper, the extent to which the excluded volume concept can simulate the in-medium effects, in particular, Pauli blocking has now been explored [29].

Calculations using the recently improved relativistic mean field (RMF) model, taking into account continuum effects [7,30], produce predictions somewhat below the experimental data. Incorporation of the latest QSM derived binding energy shifts [28] into this model have not yet been made.

While at the lowest densities the results of the theoretical calculations converge towards the NSE result, the experimentally derived equilibrium constants at these lowest densities are significantly higher. This may indicate a limit in the experiment and inclusion of a noncoalescence source of the alpha particles. Alternatively additional contributions to the alpha yield resulting from quartetting correlations which favor boson condensation, not treated in the models, might be indicated [31]. Further investigations of this region might prove fruitful.

Summary and conclusions.—Calculated equilibrium constants for specific cluster formation should be independent of n/p ratios and numbers or types of other species included. Even so, reported model calculations of the equilibrium constant for alpha formation in low density nuclear matter vary by about 2 orders of magnitude in the density and temperature region explored by the data presented in this Letter. These new experimental data for these equilibrium constants provide important constraints on the low density equations of state. The use of the NSE which neglects in-medium effects is clearly excluded as are several other models. While it is possible that these models might be improved, the data strongly indicate that accounting for in-medium effects, as in the semiempirical excluded volume approximation [8] or the more sophisticated QSM approach [28,32], is required. This is particularly evidenced by the density range of 0.01 to 0.03 nuc/fm^3 in the present data.

We recall again that details of the low density composition can be important in modeling supernova evolution and neutron star properties [6,8,33]. As emphasized in this Letter, mistakes in $K_c(\alpha)$ translate into errors not only in the yields of alpha particles but also in the yields of all competing species, regardless of the completeness with which those other species are included. The errors on the equilibrium yields of heavier species will increase with increasing mass.

[1] B. A. Li, L. W. Chen, and C. M. Ko, Phys. Rep. **464**, 113 (2008).

[2] H. Shen, H. Toki, K. Oyamatsu, and K. Sumiyoshi, Nucl. Phys. **A637**, 435 (1998); , Prog. Theor. Phys. **100**, 1013 (1998).

[3] J. M. Lattimer and F. D. Swesty, Nucl. Phys. **A535**, 331 (1991).

[4] K. Sumiyoshi, S. Yamada, H. Suzuki, H. Shen, S. Chiba, and H. Toki, Astrophys. J. **629**, 922 (2005).

[5] C. J. Horowitz and A. Schwenk, Nucl. Phys. **A776**, 55 (2006).

[6] K. Sumiyoshi and G. Röpke, Phys. Rev. C **77**, 055804 (2008).

[7] S. Typel, G. Röpke, T. Klahn, D. Blaschke, and H. H. Wolter, Phys. Rev. C **81**, 015803 (2010).

[8] M. Hempel and J. Schaffner-Bielich, Nucl. Phys. **A837**, 210 (2010).

[9] G. Shen, C. J. Horowitz, and S. Teige, Phys. Rev. C **83**, 035802 (2011).

[10] G. Shen, C. J. Horowitz, and E. O'Connor, Phys. Rev. C **83**, 065808 (2011).

[11] S. Kowalski et al., Phys. Rev. C **75**, 014601 (2007).

[12] J. B. Natowitz et al., Phys. Rev. Lett. **104**, 202501 (2010).

[13] M. B. Tsang, W. A. Friedman, C. K. Gelbke, W. G. Lynch, G. Verde, and H. S. Xu, Phys. Rev. C **64**, 041603 (2001).

[14] S. R. Souza, M. B. Tsang, R. Donangelo, W. G. Lynch, and A. W. Steiner, Phys. Rev. C **78**, 014605 (2008).

[15] S. Wuenschel et al., Nucl. Instrum. Methods Phys. Res., Sect. A **604**, 578 (2009).

[16] L. Qin, Ph.D. thesis, Texas A & M University, 2008, http://hdl.handle.net/1969.1/ETD-TAMU-2008-12-173.

[17] K. Hagel et al., Phys. Rev. C **62**, 034607 (2000).

[18] R. Wada et al., Phys. Rev. C **39**, 497 (1989).

[19] R. Wada et al., Phys. Rev. C **69**, 044610 (2004).

[20] A. Z. Mekjian, Phys. Rev. C **17**, 1051 (1978); Phys. Rev. Lett. **38**, 640 (1977).

[21] W. Bauer, Phys. Rev. C **51**, 803 (1995).

[22] H. Zheng and A. Bonasera, Phys. Lett. B **696**, 178 (2011).

[23] S. Albergo, S. Costa, E. Costanzo and A. Rubbino, Nuovo Cimento A **89**, 1 (1985).

[24] A. Kolomiets, V. M. Kolomietz, and S. Shlomo, Phys. Rev. C **55**, 1376 (1997).

[25] S. Shlomo, G. Röpke, J. B. Natowitz, L. Qin, K. Hagel, R. Wada, and A. Bonasera, Phys. Rev. C **79**, 034604 (2009).

[26] T. C. Awes, G. Poggi, C. K. Gelbke, B. B. Back, B. G. Glagola, H. Breuer and V. E. Viola, Jr., Phys. Rev. C **24**, 89 (1981).

[27] I. Cervesato, E. Fabrici, E. Gadioli, E. Gadioli-Erba, and M. Galmarini, Phys. Rev. C **45**, 2369 (1992).

[28] G. Röpke, Nucl. Phys. **A867**, 66 (2011).

[29] M. Hempel, J. Schaffner-Bielich, S. Typel, and G. Röpke, Phys. Rev. C **84**, 055804 (2011).

[30] M. D. Voskresenskaya and S. Typel, arXiv:1201.1078.

[31] G. Röpke, A. Schnell, P. Schuck, and P. Nozieres, Phys. Rev. Lett. **80**, 3177 (1998).

[32] G. Röpke, Phys. Rev. C **79**, 014002 (2009).

[33] E. O. Connor and C. D. Ott, Classical Quantum Gravity **27**, 114103 (2010).